

Fair Distillation: Teaching Fairness from Biased Teachers in Medical Imaging

Milad Masroor^{1*} Tahir Hassan^{1*} Yu Tian² Kevin Wells¹
David Rosewarne^{1,3} Thanh-Toan Do⁴ Gustavo Carneiro¹

¹ CVSSP, PAI, University of Surrey, UK

² University of Pennsylvania, USA

³ Royal Wolverhampton Hospitals NHS Trust, UK

⁴ Department of Data Science and AI, Monash University, Australia

Abstract

Deep learning has achieved remarkable success in image classification and segmentation tasks. However, fairness concerns persist, as models often exhibit biases that disproportionately affect demographic groups defined by sensitive attributes such as race, gender, or age. Existing bias-mitigation techniques, including Subgroup Re-balancing, Adversarial Training, and Domain Generalization, aim to balance accuracy across demographic groups, but often fail to simultaneously improve overall accuracy, group-specific accuracy, and fairness due to conflicts among these interdependent objectives. We propose the **Fair Distillation (FairDi)** method, a novel fairness approach that decomposes these objectives by leveraging biased “teacher” models, each optimized for a specific demographic group. These teacher models then guide the training of a unified “student” model, which distills their knowledge to maximize overall and group-specific accuracies, while minimizing inter-group disparities. Experiments on medical imaging datasets show that FairDi achieves significant gains in both overall and group-specific accuracy, along with improved fairness, compared to existing methods. FairDi is adaptable to various medical tasks, such as classification and segmentation, and provides an effective solution for equitable model performance.

1. Introduction

In recent years, deep learning models have made remarkable progress, offering automated solutions for tasks such as classification and segmentation. However, as these models transition into practice, concerns regarding fairness have emerged [3, 5, 20, 37, 40]. Machine learning models, particularly those used in healthcare, have been shown to exhibit

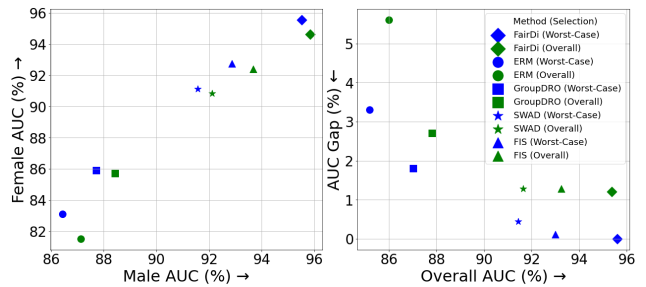


Figure 1. Performance comparison of models (ERM [57], GroupDRO [46], SWAD [2], FIS [31], and our FairDi) on the HAM10000 dataset [56] for benign/malignant classification by gender. The left panel shows group-specific AUCs (Male and Female), and the right panel plots fairness (AUC Gap) vs. Overall AUC. Each model’s Pareto front includes two points: one maximizing worst-group AUC, the other maximizing overall AUC. Our FairDi achieves the best balance with high overall AUC, low AUC Gap, and robust group-specific AUCs.

biases toward demographic groups defined by sensitive attributes such as race, gender, and age [7, 13, 64]. These biases can lead to unfair treatment of specific groups, exacerbating existing disparities. Addressing these biases is not only a technical challenge but also a moral and ethical imperative to ensure equitable healthcare for all individuals.

Current bias mitigation approaches [2, 8, 16, 33, 39, 46, 48, 52, 63] aim to reduce performance disparities across sensitive groups by modifying the training process or adjusting data distributions. These methods typically seek to maximize empirical accuracy for each sensitive group, while also improving overall accuracy and minimizing accuracy gaps between groups. Consequently, they can be formulated as multi-objective optimization problems [35], with solutions designed to achieve optimal trade-offs among conflicting objectives. These trade-offs form a set of non-dominated solutions, which are superior to all other solutions in the search space but cannot be further improved

*First two authors contributed equally to this work.

in one objective without compromising another. In this context, each fairness method generates a unique Pareto front, representing its best possible balance among objectives such as overall accuracy and inter-group fairness [35, 36, 64].

Fig. 1 compares fairness methods ERM [57], GroupDRO [46], SWAD [2], FIS [31], and our FairDi on the HAM10000 dataset [56] for benign/malignant classification by gender. The left panel illustrates group-specific AUCs (Male and Female), while the right panel plots AUC Gap versus Overall AUC. Each model’s Pareto front includes points for maximizing either worst-group or overall AUC, demonstrating trade-offs between fairness and accuracy. Unlike prior methods, which typically sacrifice overall or group-specific AUC for fairness, FairDi applies a novel decomposed optimization of the Pareto front, allowing it to achieve a superior balance, with high overall AUC, low AUC Gap, and robust group-specific AUCs, outperforming other methods on these metrics.

In this paper, we introduce the first fairness method, titled **Fair Distillation (FairDi)**, which is specifically designed to decompose the objectives of maximizing accuracy for each sensitive group from maximizing overall accuracy and minimizing inter-group accuracy gaps. This objective decomposition is achieved in two stages: first, we train highly biased models, each optimized to maximize accuracy within a specific sensitive group. These models then serve as “teachers” for a unified “student” model, which distills knowledge from the biased “teachers”, while simultaneously training to maximize overall accuracy and reduce accuracy gaps across groups, effectively balancing fairness and performance. The main contributions of this paper are:

- Introduction of the first fairness method, called FairDi, that decomposes accuracy maximization for each sensitive group from overall accuracy maximization and inter-group accuracy gap minimization, with a teacher-student model, where biased teachers are trained for specific groups, while a single student distills their knowledge, maximizing overall accuracy and reducing accuracy gaps across groups;
- Proposal of a new teacher-student training algorithm that is highly adaptable to various datasets and both classification and segmentation tasks.

Comprehensive evaluations across diverse medical imaging datasets show that FairDi significantly outperforms state-of-the-art fairness methods, achieving higher overall and group-specific accuracies while minimizing inter-group disparities. Its adaptability to various tasks, including classification and segmentation, underscores its potential to advance equitable AI in critical applications.

2. Related Work

Fairness in Artificial Intelligence (AI), particularly in healthcare, has gained increasing attention as machine learning models have been shown to exhibit biases related to sensitive attributes such as race, gender, and age [22, 26, 28–30, 32, 41, 43–45, 48–50, 54, 55, 58, 60–62, 64]. Studies by Obermeyer et al. [40] and Larrazabal et al. [24] highlight how biases in healthcare models can lead to disparities in outcomes, particularly in underrepresented populations, making fairness an essential concern in the development of AI systems for healthcare.

Bias mitigation techniques to address fairness concerns can be categorized into pre-processing, in-processing, and post-processing strategies. Pre-processing methods, like SMOTE [39], aim to re-balance data before training, while post-processing approaches [42] adjust model predictions based on sensitive attributes after training. Focusing on in-processing methods, one prominent method is Adversarial Training [21, 61], which minimizes bias by optimizing the model to perform well on the classification task while reducing its ability to predict sensitive attributes. Despite their success, these methods often encounter a trade-off between fairness and model performance [33, 63]. Another notable in-processing method is Group Distributionally Robust Optimization (GroupDRO) [46] that focuses on minimizing worst-case performance across demographic groups. Although GroupDRO ensures fairness across underperforming groups, it may reduce overall model performance [64].

Domain generalization techniques, e.g., Stochastic Weight Averaging Densely (SWAD) [2], represent in-processing methods that have shown promising results, with a training process that finds flat minima in the loss landscape. However, despite its generally robust performance, SWAD may inadvertently widen disparities between subgroups, causing it to not significantly outperform the baseline Empirical Risk Minimization (ERM) method, raising questions about its suitability as a standalone solution for fairness [64]. Another relevant in-processing method is based on representation disentanglement approaches that aim to separate sensitive attributes from task-relevant information in the learned representations. Tartaglione et al. [52] and Sarhan et al. [48] proposed disentanglement techniques that isolate sensitive attributes from the representation space, ensuring that the downstream task is unaffected by these attributes. However, while disentanglement can be effective in isolating individual sources of bias, it often underperforms in complex tasks where multiple biases coexist. This narrow focus limits generalization and efficacy, where confounding factors are deeply intertwined and challenging to separate.

Recent fairness methods introduce bias mitigation approaches to address group fairness in conjunction with over-

all accuracy. For instance, FairSeg [54] proposes Fair Error-Bound Scaling, which adjusts loss functions to focus on the hardest cases within each demographic group, ensuring equitable performance across different sensitive attributes. FairCLIP [32] reduces bias in vision-language models using an optimal transport-based method to align demographic distributions, while FairVision [31] introduces Fair Identity Scaling (FIS) to improve fairness in both 2D and 3D medical imaging. Importantly, all these methods utilize a single model, which often suffers from the conflicting objectives of group fairness and overall performance. In contrast, our approach employs cohort-specific teacher models that optimize performance independently for each cohort before distilling their knowledge into a unified student model, thus addressing fairness across groups without compromising overall performance.

Knowledge distillation has become a powerful technique in machine learning, with significant applications across various domains [11]. Firstly introduced by Bucilua et al. [1], Hinton [15], knowledge distillation is widely used for model compression [47], semi-supervised learning [53], and multi-modal learning [27]. We propose an extension of knowledge distillation to the realm of fairness in AI. By leveraging knowledge distillation to transfer cohort-specific knowledge from multiple teacher models to a unified student model, we present the first approach to utilize knowledge distillation explicitly for achieving fairness across demographic groups and optimizing model overall performance.

3. Method

Our proposed method addresses fairness in medical image analysis by implementing a student-teacher knowledge-distillation framework designed to balance cohort-specific accuracy with overall accuracy and fairness among demographic groups, as shown in Fig. 2. The approach begins by pre-training a backbone model on the full dataset using a loss function [31] that jointly optimizes the conflicting objectives of overall accuracy and fairness (Step 0). While this initial pre-training struggles to achieve an ideal balance between these objectives, it yields a robust backbone model that serves as a strong foundation for the subsequent cohort-specific teacher models and the unified student model. We then create one teacher model per demographic cohort (e.g., male or female) using the pre-trained backbone, which is greedily fine-tuned to optimize cohort-specific accuracy (Step 1). In the final stage (Step 2), our framework distills knowledge from the biased teacher models into a single student model, aiming to jointly optimize group-specific and overall accuracies together with fairness. This approach seeks to achieve the highest possible cohort-specific accuracies while also maximizing overall accuracy

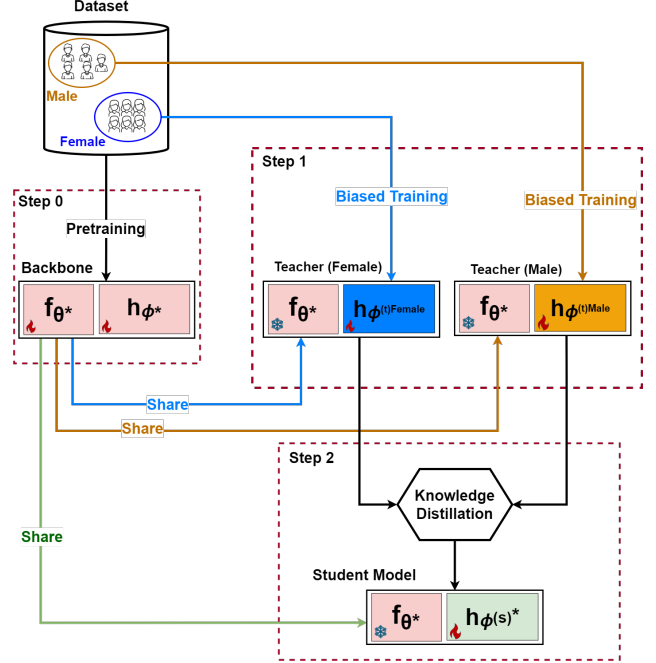


Figure 2. Diagram of the FairDi training process. After pre-training (step 0), it optimizes the teachers’ performances for their respective sensitive groups (step 1), followed by a knowledge distillation process that trains a single student to optimize overall and group-specific accuracies, while minimizing performance gap between groups (step 2). The flame symbol indicates model components to be trained during each corresponding step, while the snowflake symbol represents components that remain frozen.

and fairness for the resulting model.

3.1. Backbone Model Training (Step 0)

We assume to have a labeled dataset $\mathcal{D} = \{(x_i, y_i, a_i)\}_{i=1}^N$, where $x \in \mathcal{X} \subset \mathbb{R}^{W \times H \times R}$ is an RGB image, $y \in \mathcal{Y}$ denotes the training label, with $\mathcal{Y} \subset \{0, 1\}^Y$ for classification and $\mathcal{Y} \subset \{0, 1\}^{W \times H \times Y}$ for segmentation, and $a \in \mathcal{A} \subset \{0, \dots, A\}$ represents the value of the identity attribute (e.g., for the gender attribute, the values can be male or female) associated with the i^{th} sample of the dataset \mathcal{D} . Since we use stochastic gradient descent (or a variant) for optimization, \mathcal{D} in the formulations below denotes a mini-batch rather than the entire training set. The backbone model transforms a sample from the image space to the feature space \mathcal{F} with $f_\theta : \mathcal{X} \rightarrow \mathcal{F}$ parameterized by $\theta \in \Theta$, followed by a temperature-scaled prediction layer, defined by $h_{\phi, \tau} : \mathcal{F} \rightarrow [0, 1]^Y$ for classification and $h_{\phi, \tau} : \mathcal{F} \rightarrow [0, 1]^{W \times H \times Y}$ for segmentation, and parameterized by weights $\phi \in \Phi$ and temperature $\tau \in \mathcal{T} \subset \mathbb{R}$. This temperature modifies the final softmax function as follows $\text{softmax}(l(y), \tau) = \exp(l(y)/\tau) / \sum_{y'} \exp(l(y'), \tau)$, where $l(y)$ denotes the logit for class y – when omitted

in the following equations, assume $\tau = 1$. The backbone model and classification layer are trained using the Fair Identity Scaling (FIS) loss function [31], which is designed to balance individual and group-level fairness, with

$$\theta^*, \phi^* = \arg \min_{\theta, \phi} \frac{1}{N} \sum_{(x, y, a) \in \mathcal{D}} w(x, y, a, c) \times \ell(h_\phi(f_\theta(x)), y), \quad (1)$$

where $\ell(h_\phi(f_\theta(x)), y)$ is the classification loss and $w(x, y, a, c) = ((1 - c) \times s^I(x, y) + c \times s^G(a))$, with $s^I(x, y) = \frac{\exp(\ell(h_\phi(f_\theta(x)), y))}{\sum_{(\tilde{x}, \tilde{y}, \tilde{a}) \in \mathcal{D}} \exp(\ell(h_\phi(f_\theta(\tilde{x})), \tilde{y}))}$ representing the individual scaling weight that gives higher weight to samples that are challenging for the model, $s^G(a) = \frac{\exp(o(\mathcal{L}, \mathcal{L}_a))}{\sum_{g \in \mathcal{A}} \exp(o(\mathcal{L}, \mathcal{L}_g))}$ denoting the group scaling weight that promotes balanced learning across groups by computing the optimal transport function $o(\mathcal{L}, \mathcal{L}_g)$ that measures the distance between group loss distribution $\mathcal{L}_g = \{\ell(h_\phi(f_\theta(x)), y)\}_{(x, y, a) \in \mathcal{D} | a=g}$ and the overall loss distribution $\mathcal{L} = \{\ell(h_\phi(f_\theta(x)), y)\}_{(x, y, a) \in \mathcal{D}}$, and $c \in [0, 1]$ being a hyper-parameter controlling the balance between individual and group scaling weights. The value of c controls whether training prioritizes overall accuracy ($c \approx 0$) or fairness ($c \approx 1$) – for this pre-training, we set $c = 0.5$ for balanced training. The loss function in (1) automatically adjusts the sample weight $w(\cdot)$ based on sample-specific and group-level losses to ensure that the backbone model learns an overall accurate and fair feature space produced by the backbone feature extractor $f_{\theta^*}(\cdot)$.

3.2. Teacher Model Training (Step 1)

The cohort-specific teacher models are formed by adding a new randomly initialized classification layer $h_{\phi_g^{(t)}}(\cdot)$, for each of the teachers $g \in \{0, \dots, A\}$, to the pre-trained backbone model $f_{\theta^*}(\cdot)$ from (1), and fine tune each model by greedily minimizing classification risk for each demographic cohort $g \in \{0, \dots, A\}$, with the following loss:

$$\phi_g^{(t)*} = \arg \min_{\phi_g^{(t)}} \frac{1}{|\mathcal{D}_g|} \sum_{(x, y, a) \in \mathcal{D}_g} w(x, y, a, c) \times \ell(h_{\phi_g^{(t)}}(f_{\theta^*}(x)), y), \quad (2)$$

where $\ell(h_\phi(f_\theta(x)), y)$ is the classification loss, $w(x, y, a, c)$ is the sample weight defined in (1) with $c = 0$ to focus exclusively on the greedy individual scaling, $\mathcal{D}_g = \{(x, y, a) | (x, y, a) \in \mathcal{D}, a = g\}$, and $|\cdot|$ is the set cardinality operator. Note that in (2), we only optimize the classification layer $h_{\phi_g^{(t)}}(\cdot)$, leaving the backbone model $f_{\theta^*}(\cdot)$ frozen. This setup allows each teacher model to achieve high accuracy for its own demographic group, which is an essential step for the knowledge distillation detailed in the next section.

3.3. Student Model Training (Step 2)

In the final step, we train a unified student model by introducing a randomly initialized classification layer, denoted $h_{\phi^{(s)}}(\cdot)$, onto the pre-trained backbone model $f_{\theta^*}(\cdot)$ from Step 0 in (1). This training minimizes the following loss function:

$$\phi^{(s)*} = \arg \min_{\phi^{(s)}} \frac{1}{N} \sum_{(x, y, a) \in \mathcal{D}} \lambda \times \tau^2 \times \mathbb{KL} [h_{\phi^{(s)}}(f_{\theta^*}(x)) || h_{\phi_a^{(t)*}, \tau}(f_{\theta^*}(x))] + (1 - \lambda) \times w(x, y, a, c) \times \ell(h_{\phi^{(s)}}(f_{\theta^*}(x)), y), \quad (3)$$

where $\mathbb{KL}[\cdot]$ measures the Kullback-Leibler divergence between the student’s and group-specific teachers’ predictions [15], $\lambda \in [0, 1]$ is a hyper-parameter to balance knowledge distillation from the group-specific models and the FIS loss, and τ is the temperature scaling to soften the teacher logits [25]. In the training of (3), we set $\lambda = 0.95$, indicating that we weight more the knowledge distillation aspect of the optimization, and $c = 0.5$, suggesting a balanced FIS training between accuracy and fairness. By combining the knowledge distillation from the teacher models with the balanced fairness-accuracy FIS loss, the student model is optimized to enhance the Pareto front achieved by FIS. This approach ensures high overall accuracy, strong group-specific performance, and fair classification across groups.

4. Experiment

We evaluate FairDi on classification and segmentation tasks to showcase its versatility. This section outlines the experimental setup, datasets, evaluation metrics, competing methods, and statistical tests, followed by classification and segmentation results and an ablation study. Finally, we compare training and testing times.

4.1. Experimental Setup

Training: The classification experiments use the ResNet18 [14] backbone. In Step 0, we use Adam optimizer, a weight decay of 1×10^{-4} , and an initial learning rate of 1×10^{-4} that is decayed by a factor of 0.1 every 10 epochs, for a total of 30 epochs. To prevent overfitting, we apply an early stopping criterion where training halts if the validation worst-case area under the receiver operating characteristic curve (AUC) does not improve over 5 consecutive epochs. For Step 1, the teacher models are initialized from this backbone, with the final classification layer being randomly initialized. For training the teacher models, we use the SGD optimizer with a momentum of 0.9. Early stopping is applied here as well, halting training if the respective cohort validation AUC does not improve over 5 consecutive epochs. For Step 2, the student model is initialized from the backbone model with a randomly

initialized classification layer, and is trained using an SGD optimizer with a momentum of 0.9. The distillation loss is configured with a temperature value of $\tau = 1.5$ in Eq. (3) to soften the teacher logits. Early stopping is applied to the student model based on the validation worst-case AUC, with training terminating if no improvement is observed over 5 epochs. We use CutMix [59] to augment the training data for the training of backbone, teacher and student models. Our experiments are conducted on a computer using one NVIDIA RTX A6000 GPU. The implementation is built on Python 3.12.7 and PyTorch 2.2.2.

The segmentation experiments utilize the TransUNET backbone, built on the ViT-B (Vision Transformer) architecture, tailored specifically for medical imaging. The model is trained using the AdamW optimizer with a learning rate of 0.01, momentum of 0.9, weight decay of 1×10^{-4} , and exponential learning rate decay. In the initial stages of training, a warmup strategy is employed to stabilize model training with the Harvard-FairSeg dataset [54]. The TransUNET model is trained for 300 epochs without early stopping, following its original implementation, ensuring robust segmentation performance. The batch size for training is set to 42. The warmup strategy is applied at the beginning of training to stabilize the models.

Datasets: For the classification task, we conduct our experiments on five medical imaging datasets that have been used to benchmark fairness methods [64]—they are: Fitzpatrick17K [12], HAM10000 [56], Papila [23], CheXpert [17], and MIMIC-CXR [19]. To ensure consistent data preparation across all datasets, we follow a standardized pre-processing approach inspired by [64]. For example, we binarize sensitive attributes (e.g., skin type, age, sex, and race) and classification labels to facilitate evaluation of demographic fairness. More specifically, HAM10000 has classes benign and malignant, and two sensitive attributes: ‘Age’ (binarized into 0 to 60 and above 60) and ‘Gender’ (Male and Female). Fitzpatrick17k has classes malignant and non-malignant, with the ‘Skin Type’ attribute binarized into one group with skin types ranging from 0 to 2, and another group with skin types above 2. The PAPIA dataset has classes healthy and glaucoma, with two sensitive attributes: ‘Age’ (binarized into 0 to 60 and above 60) and ‘Gender’ (Male and Female). The CheXpert and MIMIC-CXR has classes ‘No-Finding’ and ‘Any Finding’, with three sensitive attributes: ‘Age’ (binarized into 0 to 60 and above 60), ‘Gender’ (Male and Female), and ‘Race’ (Non-White, including Black or Asian patients, and White). Additionally, as instructed by the MedFair benchmark [64], samples with incomplete or missing data are excluded from the analysis. A more detailed description of the pre-processing is provided in Sec. 6 of the supplementary material.

For the segmentation task, we use the Harvard-FairSeg

dataset [54], which is a scanning laser ophthalmoscopy (SLO) fundus image dataset with a disc-cup segmentation task to assess the optic nerve head structures and diagnosing glaucoma in its early stage. This Harvard-FairSeg dataset has 10,000 samples collected from 10,000 unique subjects. We split the data into an 8,000 for training and a 2,000 for testing. The subjects in the dataset have a mean age of 60.3 years, with a standard deviation of 16.5 years. Six sensitive attributes—age, gender, race, ethnicity, preferred language, and marital status—are available to support fairness-focused studies. In this paper, we focus on three sensitive attributes with the highest observed group-wise discrepancies: race, gender, and ethnicity.

More details about the classification and segmentation datasets are shown in Sec. 7 in the supp. material.

Evaluation Measures and Statistical Tests: Binary classification is assessed with AUC. To evaluate fairness, we report metrics that account for performance disparities across demographics cohorts. For instance, AUC Gap [64] measures the performance difference between the highest and lowest-performing cohorts. The Worst-Case AUC [64] calculates the minimum AUC achieved among all cohorts. Another fairness measure that we present is the Equity-Scaled AUC (ES-AUC) [31], defined in Sec. 8 of the supplementary material, which adjusts the overall AUC by penalizing discrepancies between the AUCs of the cohorts. We also measure the Performance-Scaled Disparity (PSD) that evaluates fairness by comparing cohort performance relative to overall AUC—please see Sec. 8 of the supplementary material for the definition of the MeanPSD, which calculates the standard deviation of AUC scores across cohorts, and MaxPSD that calculates the maximum absolute difference between cohorts’ AUCs.

We evaluate the segmentation tasks using the Dice Similarity Coefficient [6, 51], which measures the overlap between predicted and ground truth segmentations, and the Intersection over Union (IoU) [18] that measures the ratio of the intersection to the union of the predicted and ground truth segments. In the FairSeg benchmark [54], Equity-scaled Dice (ES-Dice) and IoU (ES-IoU) modify the Dice and IoU to penalize discrepancies in performance across demographic groups by scaling the overlap scores down if subgroup performance is uneven. In essence, equity-scaled metrics reduce the overall score when there are larger performance gaps between cohorts, encouraging models to achieve consistent segmentation quality across all subgroups—please see Sec. 8 of the supplementary material for the definition of ES-Dice and ES-IoU.

As suggested in [64], we test significance by applying the Friedman test [9], followed by the Nemenyi post-hoc test [38], to detect significant performance differences between algorithms. If the Friedman test shows significance (p -value < 0.05), the Nemenyi test averages the ranks of

each algorithm across datasets. The results are displayed using Critical Difference (CD) diagrams, where algorithms connected by a line are statistically similar, while those in separate groups are significantly different.

Baselines and State-of-the-art (SOTA) Methods: We compare our proposed FairDi against several baseline and SOTA fairness methods. For the classification task, a common baseline in fairness studies is the Empirical Risk Minimization (ERM) [57], which is trained by minimizing the average classification error across the training set without accounting for demographic cohorts or sensitive attributes. While ERM optimizes overall accuracy, it overlooks group-specific biases, making it a valuable baseline for assessing fairness gaps. GroupDRO [46] is designed to minimize the worst-case loss across demographic groups. By focusing on the group with the highest training loss, GroupDRO emphasizes performance fairness, aiming to protect disadvantaged cohorts. Another baseline, SWAD [2], explores a range of flat minima in the loss landscape through dense sampling of model weights. This approach is particularly beneficial for enhancing model generalization across diverse settings, but does not directly address fairness across demographic groups. We also compare our approach to FIS [31], the SOTA fairness method that applies a scaling mechanism to adjust loss contributions based on demographic cohort performance.

We evaluate fair segmentation with the TransUNet backbone [4], which combines CNNs with transformers, leveraging self-attention for capturing long-range dependencies while preserving spatial hierarchies, making it effective for medical image segmentation. The first TransUNet-based fair segmentation method is implemented by combining it with the Adversarially Fair Representations (ADV) [33] to create unbiased representations by making it difficult to infer sensitive attributes, thus reducing bias. Another fair TransUNet method is achieved by combining it with GroupDRO [46], which improves model fairness by minimizing the maximum training loss across groups, using regularization to prevent bias toward any single group. We also compare with the SOTA TransUNet+Fair Error-Bound Scaling (FEBS) [54] that improves fairness by rescaling the loss based on each identity group’s upper training error bound.

4.2. Classification Results

Table 1 summarizes results across all datasets and sensitive attributes, where complete results are available in Table 11 of the supplementary material. FairDi achieves the highest average metrics across all measures, with an Average Overall AUC of 0.9137, outperforming FIS (0.8976), SWAD (0.8735), GroupDRO (0.8511), and ERM (0.8485), demonstrating superior robustness and consistency across sensitive attributes. In fairness metrics, FairDi attains the highest Average Minimum AUC Score (0.9050), indicating

Table 1. Summary of the evaluation and ranking of fairness models (ERM, GroupDRO, SWAD, FIS, and our FairDi) across **classification** benchmarks HAM10000 (attributes: Age, Gender), Fitzpatrick17k (attribute: Skin Type), PAPILA (attributes: Age, Gender), CheXpert (attributes: Age, Gender, Race), and MIMIC-CXR (attributes: Age, Gender, Race). We report overall AUC, minimum AUC, ES-AUC, AUC gap, MeanPSD, and MaxPSD. Best results are highlighted and detailed results are shown in Table 11 of the supplementary material.

Measures and Ranks	ERM	GroupDRO	SWAD	FIS	FairDi (Ours)
Avg. Overall AUC Score \uparrow	0.8485	0.8511	0.8735	0.8976	0.9137
Avg. Min. AUC Score \uparrow	0.8082	0.8127	0.8350	0.8815	0.9050
Avg. ES-AUC Score \uparrow	0.8264	0.8253	0.8474	0.8864	0.9062
Avg. AUC Gap Score \downarrow	0.0589	0.0710	0.0683	0.0249	0.0166
Avg. MeanPSD Score \downarrow	0.0379	0.0440	0.0410	0.0141	0.0091
Avg. MaxPSD Score \downarrow	0.0758	0.0881	0.0820	0.0282	0.0182
Avg. Overall AUC Rank \downarrow	3.55	4.45	2.55	2.91	1.55
Avg. Min. AUC Rank \downarrow	3.91	4.36	2.64	2.73	1.36
Avg. ES-AUC Rank \downarrow	3.82	4.45	2.45	2.73	1.55
Avg. AUC Gap Rank \downarrow	3.00	3.55	3.27	3.00	2.18
Avg. MeanPSD Rank \downarrow	3.00	3.55	3.27	3.00	2.18
Avg. MaxPSD Rank \downarrow	3.00	3.55	3.27	3.00	2.18

Table 2. Summary of the evaluation and ranking of fairness models (TransUNet, TransUNet+ADV, TransUNet+GroupDRO, TransUNet+FEBS, and our TransUNet+FairDi) across the **segmentation** of optic cup and rim on the Harvard-FairSeg dataset, with race, gender and ethnicity sensitive attributes. We report Overall ES-Dice, Overall Dice, Overall ES-IoU, and Overall IoU. Best results are highlighted and detail results are shown in Tabs. 12 to 14 at the supplementary material.

Measures and Ranks	TransUNet	TransUNet + ADV	TransUNet + GroupDRO	TransUNet + FEBS	TransUNet + FairDi (Ours)
Avg. Overall ES-Dice Score \uparrow	0.7955	0.7873	0.7956	0.7966	0.8062
Avg. Overall Dice Score \uparrow	0.8204	0.8112	0.8193	0.8204	0.8260
Avg. Overall ES-IoU Score \uparrow	0.6871	0.6767	0.6870	0.6889	0.7002
Avg. Overall IoU Score \uparrow	0.7119	0.7003	0.7106	0.7124	0.7209
Avg. Overall ES-Dice Rank \downarrow	3.17	4.67	3.00	3.00	1.17
Avg. Overall Dice Rank \downarrow	3.00	4.83	3.50	2.67	1.00
Avg. Overall ES-IoU Rank \downarrow	3.17	4.50	3.67	2.67	1.00
Avg. Overall IoU Rank \downarrow	2.67	4.83	3.83	2.67	1.00

robustness across the most challenging subgroup, compared to FIS (0.8815) and others. FairDi also leads in Average ES-AUC Score at 0.9062, outperforming FIS (0.8864), SWAD (0.8474), GroupDRO (0.8253), and ERM (0.8264). FairDi achieves the lowest Average AUC Gap Score of 0.0166, indicating minimal performance discrepancy across groups, while FIS follows with 0.0249. SWAD, GroupDRO, and ERM show significantly higher AUC Gaps, highlighting FairDi’s effectiveness in reducing group disparities. Similarly, FairDi achieves the lowest MeanPSD (0.0091) and MaxPSD (0.0182) scores, reflecting its ability to provide fairer outcomes across demographics.

Fig. 3 shows the Nemenyi post-hoc test results on Overall AUC, Worst-case AUC, ES-AUC, AUC Gap, Mean PSD and Max PSD settings with raw data in Tab. 11 of the supplementary material. Our FairDi is the highest ranked

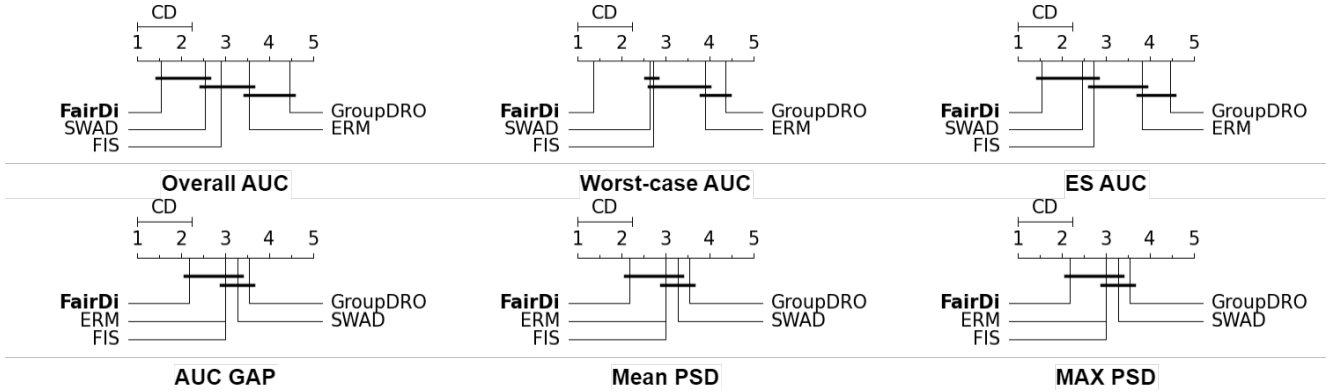


Figure 3. Performance of fairness algorithms for classification across all datasets as average rank CD diagrams. Our FairDi is the highest ranked method for all settings, being significantly better than most methods, and for the worst-case AUC, it is the single best method.

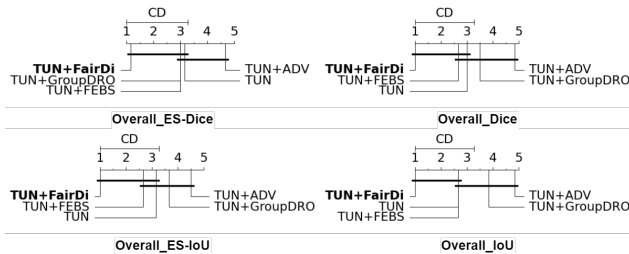


Figure 4. Performance of fairness segmentation algorithms shown with average rank CD diagrams. FairDi consistently outperforms most methods, ranking the highest in all settings. In this figure, TUN stands for TransUNet

method for all settings, where for most settings, it is significantly better than between 1 to all four competing methods. It is worth noting that for the worst-case AUC, our method is significantly better than all others. These results demonstrate FairDi’s ability to enhance both classification accuracy and fairness, significantly reducing performance gaps across demographic subgroups.

4.3. Segmentation Results

Table 2 shows a summary of the results of TransUNet [4], TransUNet+ADV [33], TransUNet+GroupDRO [46], TransUNet+FEBS [54], and our proposed TransUNet+FairDi across race, gender and ethnicity sensitive attributes, where the complete results are available in Tabs. 12 to 14 of the supplementary material. FairDi achieves the highest average metrics across all measures, with an Average Overall Dice of 0.8260, which is superior to FEBS (0.8204), GroupDRO (0.8193), ADV (0.8112), and TransUNet (0.8204). Regarding fairness metrics, FairDi achieves an Overall ES-Dice of 0.8062, outperforming FEBS (0.7966), GroupDRO (0.7956), ADV (0.7873), and TransUNet (0.7955). Similar results are observed for IoU and ES-IoU, demonstrating the ability of our approach achieve fairer segmentation across

various cohorts.

The Nemenyi post-hoc test results on Overall Dice, Overall ES-Dice, Overall IoU, Overall ES-IoU shown in Fig. 4, with raw data in Tabs. 12 to 14 at the supplementary material, demonstrate that our FairDi is the highest ranked method for all settings. Note that for most settings, it is significantly better than between 1 and 2 competing methods. These results confirm FairDi’s ability to improve segmentation accuracy and fairness.

4.4. Ablation Study

In this ablation study, we explore the technical contributions of our FairDi model, on two classification datasets, to understand their impact on accuracy and fairness. Tab. 3 presents the results across the HAM10000 and PAPILA datasets, focusing on Gender as the sensitive attribute. We start from the baseline ERM model (ResNet18) trained with binary cross entropy (BCE) loss [64], which has moderate Overall AUC scores of 0.8890 on HAM10000 and 0.8433 on PAPILA. Integrating CutMix [59], the Overall AUC results improve to 0.8952 on HAM10000 and 0.9142 on PAPILA. However, this accuracy enhancement results in a larger AUC Gap, particularly on PAPILA, which reaches 0.1500. Replacing BCE with FIS loss [31], increases Overall AUC to 0.9174 on HAM10000 and 0.8938 on PAPILA and substantially reduces AUC Gap to 0.0071 on HAM10000 and 0.0331 on PAPILA, showing a better balance between accuracy and fairness. The combination of FIS Loss with CutMix leads to further improvements, reaching an Overall AUC of 0.9300 on HAM10000 and 0.9391 on PAPILA and further AUC Gap reductions to 0.0011 on HAM10000 and 0.0285 on PAPILA. This configuration achieves high ES-AUC and low MeanPSD and MaxPSD values, indicating a favorable balance between accuracy and fairness. This forms the backbone model from Step 0, explained in Sec. 3.1.

Step 1, explained in Sec. 3.2, consists of training group-

Table 3. Ablation study on HAM10000 (with attribute Gender) and PAPILA (with attribute Gender). Starting from ERM, followed by ERM + CutMix, FIS, FIS + CutMix (Step 0), FairDi-Teacher (Female - Step 1), FairDi-Teacher (Male - Step 1), and FairDi-Student (Step 2).

Dataset (Attribute)	Metric	ERM	ERM + CutMix	FIS	FIS + CutMix (Step 0)	FairDi-Teacher (Female - Step 1)	FairDi-Teacher (Male - Step 1)	FairDi-Student (Step 2)
HAM10000 (Gender)	Overall AUC \uparrow	0.8890	0.8952	0.9174	0.9300	0.9420	0.9502	0.9560
	Female AUC \uparrow	0.8826	0.8785	0.9151	0.9276	0.9585	0.9475	0.9554
	Male AUC \uparrow	0.8956	0.9157	0.9222	0.9287	0.9300	0.9510	0.9553
	AUC Gap \downarrow	0.0130	0.0372	0.0071	0.0011	0.0285	0.0035	0.000029
	ES-AUC \uparrow	0.8833	0.8789	0.9142	0.9283	0.9288	0.9485	0.9553
	MeanPSD \downarrow	7.31×10^{-3}	2.08×10^{-2}	3.87×10^{-3}	5.77×10^{-4}	1.51×10^{-2}	1.84×10^{-3}	1.52×10^{-5}
	MaxPSD \downarrow	1.46×10^{-2}	4.16×10^{-2}	7.74×10^{-3}	1.15×10^{-3}	3.03×10^{-2}	3.68×10^{-3}	3.03×10^{-5}
PAPILA (Gender)	Overall AUC \uparrow	0.8433	0.9142	0.8938	0.9391	0.9315	0.9395	0.9572
	Female AUC \uparrow	0.8447	0.9714	0.8905	0.9471	0.9515	0.9027	0.9508
	Male AUC \uparrow	0.8267	0.8214	0.9236	0.9186	0.8897	0.9841	0.9857
	AUC Gap \downarrow	0.0180	0.1500	0.0331	0.0285	0.0618	0.0814	0.0349
	ES-AUC \uparrow	0.8358	0.8504	0.8792	0.9259	0.9036	0.9028	0.9408
	MeanPSD \downarrow	1.07×10^{-2}	8.2×10^{-2}	1.85×10^{-2}	1.52×10^{-2}	3.32×10^{-2}	4.33×10^{-2}	1.82×10^{-2}
	MaxPSD \downarrow	2.13×10^{-2}	1.64×10^{-1}	3.70×10^{-2}	3.03×10^{-2}	6.63×10^{-2}	8.66×10^{-2}	3.64×10^{-2}

specific FairDi-teacher models, which have high group-specific overall AUC scores, with Female AUC reaching 0.9585 and Male AUC reaching 0.9510 on HAM10000, and similar performances on PAPILA (Female AUC of 0.9515 and Male AUC of 0.9841). However, these biased models also introduce larger AUC Gap values (0.0285 on HAM10000 and 0.0814 on PAPILA) due to the inherent performance discrepancy between the cohort-specific models. This suggests that while group-specific performances are strong, fairness is sacrificed.

The final knowledge distillation (from group-specific teacher models) and accuracy-fairness balanced training of the student model during Step 2, explained in Sec. 3.3, produces the FairDi-student model, which achieves an Overall AUC of 0.9560 on HAM10000 and 0.9572 on PAPILA. Both Female and Male AUCs remain high, while the model minimizes the AUC Gap to just 0.000029 on HAM10000 and 0.0349 on PAPILA. These results indicate a significant reduction in cohort-specific performance disparities compared to the biased teacher models, demonstrating the effectiveness of our FairDi design in balancing cohort-specific performance with overall accuracy and fairness.

4.5. Training and Testing Running Times

For the HAM10000 dataset with gender-sensitive attribute, the training times for ERM, SWAD, GroupDRO, and FIS were 19.75, 28.78, 19.12, and 17.56 minutes, respectively. In comparison, the FairDi method’s total training time is structured across the following multiple steps: Backbone Model Training (Step 0) takes 17.56 minutes, Teacher (Female) Model Training (Step 1) takes 5.53 minutes, Teacher (Male) Model Training (Step 1) takes 4.26 minutes, and Student Model Training (Step 2) takes 16.96 minutes, resulting in a combined training time of ≈ 40 minutes, assuming that the two teachers can be trained in parallel. The testing time for ERM, SWAD, GroupDRO, FIS, and FairDi is identical at 0.033 seconds per image. In terms of memory footprint, the backbone model contains a total of $\approx 11\text{M}$

parameters, all of which are trainable at Step 0 of the training. The classification layers of the female and male teacher models introduce $\approx 0.5\text{K}$ (each) new parameters trainable at Step 1 of the training. Similarly, the student model adds another $\approx 0.5\text{K}$ new parameters at the classification layer, with the same $\approx 11\text{M}$ non-trainable parameters from the backbone model.

5. Conclusion

In this work, we introduced FairDi, a novel fairness method that tackles the challenging trade-offs between accuracy, subgroup-specific performance, and fairness in medical imaging. Unlike traditional fairness approaches that attempt to balance these competing goals within a single model, FairDi leverages the strengths of biased teacher models trained specifically for sensitive subgroups. This unique strategy allows the unified student model to distill the teacher models’ knowledge and achieve high overall accuracy, while reducing performance disparities across demographic groups.

Our extensive evaluations across multiple medical imaging datasets demonstrate that FairDi consistently outperforms current fairness methods, achieving both high accuracy and fairness. The experimental results highlight FairDi’s ability to narrow the AUC gap between advantaged and disadvantaged subgroups, while also minimizing performance-scaled disparity (PSD), a crucial metric for real-world clinical relevance. Furthermore, by distilling knowledge from subgroup-optimized teachers, FairDi not only enhances the interpretability of fairness outcomes but also sets a new standard for equitable model performance in healthcare.

The flexibility and adaptability of FairDi make it applicable to a range of medical tasks, including classification and segmentation, underscoring its potential impact on the design of fair AI systems in critical domains. As healthcare increasingly adopts AI solutions, FairDi stands as a promising pathway toward ethical, inclusive, and high-performing

models that prioritize equitable outcomes for all patients. We hope that this work paves the way for further advancements in fairness-centered AI, inspiring new strategies that embrace the complexities of fairness without sacrificing performance.

References

- [1] Cristian Buciluă, Rich Caruana, and Alexandru Niculescu-Mizil. Model compression. In *Proceedings of the 12th ACM SIGKDD international conference on Knowledge discovery and data mining*, pages 535–541, 2006. 3
- [2] Junbum Cha, Sanghyuk Chun, Kyungjae Lee, Han-Cheol Cho, Seunghyun Park, Yunsung Lee, and Sungrae Park. Swad: Domain generalization by seeking flat minima. *Advances in Neural Information Processing Systems*, 34: 22405–22418, 2021. 1, 2, 6
- [3] Irene Y Chen, Emma Pierson, Sherri Rose, Shalmali Joshi, Kadija Ferryman, and Marzyeh Ghassemi. Ethical machine learning in healthcare. *Annual review of biomedical data science*, 4(1):123–144, 2021. 1
- [4] Jieneng Chen, Yongyi Lu, Qihang Yu, Xiangde Luo, Ehsan Adeli, Yan Wang, Le Lu, Alan L Yuille, and Yuyin Zhou. Transunet: Transformers make strong encoders for medical image segmentation. *arXiv preprint arXiv:2102.04306*, 2021. 6, 7
- [5] Richard J Chen, Judy J Wang, Drew FK Williamson, Tiffany Y Chen, Jana Lipkova, Ming Y Lu, Sharifa Sahai, and Faisal Mahmood. Algorithmic fairness in artificial intelligence for medicine and healthcare. *Nature biomedical engineering*, 7(6):719–742, 2023. 1
- [6] Lee R Dice. Measures of the amount of ecologic association between species. *Ecology*, 26(3):297–302, 1945. 5, 3
- [7] Raman Dutt, Ondrej Bohdal, Sotirios A Tsaftaris, and Timothy Hospedales. Fairtune: Optimizing parameter efficient fine tuning for fairness in medical image analysis. *arXiv preprint arXiv:2310.05055*, 2023. 1
- [8] Pierre Foret, Ariel Kleiner, Hossein Mobahi, and Behnam Neyshabur. Sharpness-aware minimization for efficiently improving generalization. *arXiv preprint arXiv:2010.01412*, 2020. 1
- [9] Milton Friedman. The use of ranks to avoid the assumption of normality implicit in the analysis of variance. *Journal of the american statistical association*, 32(200):675–701, 1937. 5
- [10] Ary L Goldberger, Luis AN Amaral, Leon Glass, Jeffrey M Hausdorff, Plamen Ch Ivanov, Roger G Mark, Joseph E Mietus, George B Moody, Chung-Kang Peng, and H Eugene Stanley. Physiobank, physiotoolkit, and physionet: components of a new research resource for complex physiologic signals. *circulation*, 101(23):e215–e220, 2000. 2
- [11] Jianping Gou, Baosheng Yu, Stephen J Maybank, and Dacheng Tao. Knowledge distillation: A survey. *International Journal of Computer Vision*, 129(6):1789–1819, 2021. 3
- [12] Matthew Groh, Caleb Harris, Luis Soenksen, Felix Lau, Rachel Han, Aerin Kim, Arash Koochek, and Omar Badri. Evaluating deep neural networks trained on clinical images in dermatology with the fitzpatrick 17k dataset. In *Proceedings of the IEEE/CVF Conference on Computer Vision and Pattern Recognition*, pages 1820–1828, 2021. 5
- [13] Xiaotian Han, Jianfeng Chi, Yu Chen, Qifan Wang, Han Zhao, Na Zou, and Xia Hu. FFB: A fair fairness benchmark for in-processing group fairness methods. In *The Twelfth International Conference on Learning Representations*, 2024. 1
- [14] Kaiming He, Xiangyu Zhang, Shaoqing Ren, and Jian Sun. Deep residual learning for image recognition. In *Proceedings of the IEEE conference on computer vision and pattern recognition*, pages 770–778, 2016. 4
- [15] Geoffrey Hinton. Distilling the knowledge in a neural network. *arXiv preprint arXiv:1503.02531*, 2015. 3, 4
- [16] Badr Youbi Idrissi, Martin Arjovsky, Mohammad Pezeshki, and David Lopez-Paz. Simple data balancing achieves competitive worst-group-accuracy. In *Conference on Causal Learning and Reasoning*, pages 336–351. PMLR, 2022. 1
- [17] Jeremy Irvin, Pranav Rajpurkar, Michael Ko, Yifan Yu, Silvana Ciurea-Ilcus, Chris Chute, Henrik Marklund, Behzad Haghgoo, Robyn Ball, Katie Shpanskaya, et al. Chexpert: A large chest radiograph dataset with uncertainty labels and expert comparison. In *Proceedings of the AAAI conference on artificial intelligence*, pages 590–597, 2019. 5
- [18] Paul Jaccard. Étude comparative de la distribution florale dans une portion des alpes et des jura. *Bull Soc Vaudoise Sci Nat*, 37:547–579, 1901. 5, 3
- [19] Alistair EW Johnson, Tom J Pollard, Nathaniel R Greenbaum, Matthew P Lungren, Chih-ying Deng, Yifan Peng, Zhiyong Lu, Roger G Mark, Seth J Berkowitz, and Steven Horng. Mimic-cxr-jpg, a large publicly available database of labeled chest radiographs. *arXiv preprint arXiv:1901.07042*, 2019. 5, 2
- [20] Achuta Kadambi. Achieving fairness in medical devices. *Science*, 372(6537):30–31, 2021. 1
- [21] Byungju Kim, Hyunwoo Kim, Kyungsu Kim, Sungjin Kim, and Junmo Kim. Learning not to learn: Training deep neural networks with biased data. In *Proceedings of the IEEE/CVF conference on computer vision and pattern recognition*, pages 9012–9020, 2019. 2
- [22] Michael P Kim, Amirata Ghorbani, and James Zou. Multi-accuracy: Black-box post-processing for fairness in classification. In *Proceedings of the 2019 AAAI/ACM Conference on AI, Ethics, and Society*, pages 247–254, 2019. 2
- [23] Oleksandr Kovalyk, Juan Morales-Sánchez, Rafael Verdú-Monedero, Inmaculada Sellés-Navarro, Ana Palazón-Cabanes, and José-Luis Sancho-Gómez. Papila: Dataset with fundus images and clinical data of both eyes of the same patient for glaucoma assessment. *Scientific Data*, 9(1):291, 2022. 5
- [24] Agostina J Larrazabal, Nicolás Nieto, Victoria Peterson, Diego H Milone, and Enzo Ferrante. Gender imbalance in medical imaging datasets produces biased classifiers for computer-aided diagnosis. *Proceedings of the National Academy of Sciences*, 117(23):12592–12594, 2020. 2

- [25] Xin-Chun Li, Wen-Shu Fan, Shaoming Song, Yinchuan Li, Shao Yunfeng, De-Chuan Zhan, et al. Asymmetric temperature scaling makes larger networks teach well again. *Advances in neural information processing systems*, 35:3830–3842, 2022. 4
- [26] Pranay K Lohia, Karthikeyan Natesan Ramamurthy, Manish Bhide, Diptikalyan Saha, Kush R Varshney, and Ruchir Puri. Bias mitigation post-processing for individual and group fairness. In *Icassp 2019-2019 IEEE international conference on acoustics, speech and signal processing (icassp)*, pages 2847–2851. IEEE, 2019. 2
- [27] Jiasen Lu, Dhruv Batra, Devi Parikh, and Stefan Lee. Vilbert: Pretraining task-agnostic visiolinguistic representations for vision-and-language tasks. *Advances in neural information processing systems*, 32, 2019. 3
- [28] Yan Luo, Min Shi, Yu Tian, Tobias Elze, and Mengyu Wang. Harvard glaucoma detection and progression: A multimodal multitask dataset and generalization-reinforced semi-supervised learning. In *Proceedings of the IEEE/CVF International Conference on Computer Vision*, pages 20471–20482, 2023. 2
- [29] Yan Luo, Yu Tian, Min Shi, Tobias Elze, and Mengyu Wang. Eye fairness: A large-scale 3d imaging dataset for equitable eye diseases screening and fair identity scaling. *arXiv preprint arXiv:2310.02492*, 2023.
- [30] Yan Luo, Yu Tian, Min Shi, Tobias Elze, and Mengyu Wang. Harvard glaucoma fairness: A retinal nerve disease dataset for fairness learning and fair identity normalization. *arXiv preprint arXiv:2306.09264*, 2023. 2
- [31] Yan Luo, Muhammad Osama Khan, Yu Tian, Min Shi, Zehao Dou, Tobias Elze, Yi Fang, and Mengyu Wang. Fairvision: Equitable deep learning for eye disease screening via fair identity scaling, 2024. 1, 2, 3, 4, 5, 6, 7
- [32] Yan Luo, Min Shi, Muhammad Osama Khan, Muhammad Muneeb Afzal, Hao Huang, Shuaihang Yuan, Yu Tian, Luo Song, Ava Kouhana, Tobias Elze, et al. Fairclip: Harnessing fairness in vision-language learning. In *Proceedings of the IEEE/CVF Conference on Computer Vision and Pattern Recognition*, pages 12289–12301, 2024. 2, 3
- [33] David Madras, Elliot Creager, Toniann Pitassi, and Richard Zemel. Learning adversarially fair and transferable representations. In *International Conference on Machine Learning*, pages 3384–3393. PMLR, 2018. 1, 2, 6, 7
- [34] Roman C Maron, Michael Weichenthal, Jochen S Utikal, Achim Hekler, Carola Berking, Axel Hauschild, Alexander H Enk, Sebastian Haferkamp, Joachim Klode, Dirk Schadendorf, et al. Systematic outperformance of 112 dermatologists in multiclass skin cancer image classification by convolutional neural networks. *European Journal of Cancer*, 119:57–65, 2019. 1
- [35] Natalia Martinez, Martin Bertran, and Guillermo Sapiro. Minimax pareto fairness: A multi objective perspective. In *International conference on machine learning*, pages 6755–6764. PMLR, 2020. 1, 2
- [36] Andreu Mas-Colell, Michael D. Whinston, Jerry R. Green, et al. *Microeconomic theory, volume 1*. Oxford university press New York, 1995. 2
- [37] Ninareh Mehrabi, Fred Morstatter, Nripsuta Saxena, Kristina Lerman, and Aram Galstyan. A survey on bias and fairness in machine learning. *ACM computing surveys (CSUR)*, 54(6):1–35, 2021. 1
- [38] Peter Bjorn Nemenyi. *Distribution-free multiple comparisons*. Princeton University, 1963. 5
- [39] V Chawla Nitesh. Smote: synthetic minority over-sampling technique. *J Artif Intell Res*, 16(1):321, 2002. 1, 2
- [40] Ziad Obermeyer, Brian Powers, Christine Vogeli, and Sendhil Mullainathan. Dissecting racial bias in an algorithm used to manage the health of populations. *Science*, 366(6464):447–453, 2019. 1, 2
- [41] Sungho Park, Jewook Lee, Pilhyeon Lee, Sunhee Hwang, Dohyung Kim, and Hyeran Byun. Fair contrastive learning for facial attribute classification. In *Proceedings of the IEEE/CVF Conference on Computer Vision and Pattern Recognition*, pages 10389–10398, 2022. 2
- [42] Geoff Pleiss, Manish Raghavan, Felix Wu, Jon Kleinberg, and Kilian Q Weinberger. On fairness and calibration. *Advances in neural information processing systems*, 30, 2017. 2
- [43] Novi Quadrianto, Viktoriia Sharmanska, and Oliver Thomas. Discovering fair representations in the data domain. In *Proceedings of the IEEE/CVF conference on computer vision and pattern recognition*, pages 8227–8236, 2019. 2
- [44] Vikram V Ramaswamy, Sunnie SY Kim, and Olga Russakovsky. Fair attribute classification through latent space de-biasing. In *Proceedings of the IEEE/CVF conference on computer vision and pattern recognition*, pages 9301–9310, 2021.
- [45] Yuji Roh, Kangwook Lee, Steven Whang, and Changho Suh. Fr-train: A mutual information-based approach to fair and robust training. In *International Conference on Machine Learning*, pages 8147–8157. PMLR, 2020. 2
- [46] Shiori Sagawa, Pang Wei Koh, Tatsunori B Hashimoto, and Percy Liang. Distributionally robust neural networks for group shifts: On the importance of regularization for worst-case generalization. *arXiv preprint arXiv:1911.08731*, 2019. 1, 2, 6, 7
- [47] V Sanh. Distilbert, a distilled version of bert: Smaller, faster, cheaper and lighter. *arXiv preprint arXiv:1910.01108*, 2019. 3
- [48] Mhd Hasan Sarhan, Nassir Navab, Abouzar Eslami, and Shadi Albarqouni. Fairness by learning orthogonal disentangled representations. In *Computer Vision—ECCV 2020: 16th European Conference, Glasgow, UK, August 23–28, 2020, Proceedings, Part XXIX 16*, pages 746–761. Springer, 2020. 1, 2
- [49] Min Shi, Yan Luo, Yu Tian, Lucy Q Shen, Tobias Elze, Nazlee Zebardast, Mohammad Eslami, Saber Kazeminasab, Michael V Boland, David S Friedman, et al. Equitable artificial intelligence for glaucoma screening with fair identity normalization. *medRxiv*, pages 2023–12, 2023.
- [50] Min Shi, Muhammad Muneeb Afzal, Hao Huang, Congcong Wen, Yan Luo, Muhammad Osama Khan, Yu Tian, Leo Kim, Tobias Elze, Yi Fang, et al. Equitable deep learning for

- diabetic retinopathy detection using multi-dimensional retinal imaging with fair adaptive scaling: a retrospective study. *medRxiv*, pages 2024–04, 2024. [2](#)
- [51] Thorvald Sorensen. A method of establishing groups of equal amplitude in plant sociology based on similarity of species content and its application to analyses of the vegetation on danish commons. *Biologiske skrifter*, 5:1–34, 1948. [5](#), [3](#)
- [52] Enzo Tartaglione, Carlo Alberto Barbano, and Marco Grangetto. End: Entangling and disentangling deep representations for bias correction. In *Proceedings of the IEEE/CVF conference on computer vision and pattern recognition*, pages 13508–13517, 2021. [1](#), [2](#)
- [53] Antti Tarvainen and Harri Valpola. Mean teachers are better role models: Weight-averaged consistency targets improve semi-supervised deep learning results. *Advances in neural information processing systems*, 30, 2017. [3](#)
- [54] Yu Tian, Min Shi, Yan Luo, Ava Kouhana, Tobias Elze, and Mengyu Wang. Fairseg: A large-scale medical image segmentation dataset for fairness learning using segment anything model with fair error-bound scaling. In *The Twelfth International Conference on Learning Representations*, 2024. [2](#), [3](#), [5](#), [6](#), [7](#), [1](#)
- [55] Yu Tian, Congcong Wen, Min Shi, Muhammad Muneeb Afzal, Hao Huang, Muhammad Osama Khan, Yan Luo, Yi Fang, and Mengyu Wang. Fairdomain: Achieving fairness in cross-domain medical image segmentation and classification. *arXiv preprint arXiv:2407.08813*, 2024. [2](#)
- [56] Philipp Tschandl, Cliff Rosendahl, and Harald Kittler. The ham10000 dataset, a large collection of multi-source dermatoscopic images of common pigmented skin lesions. *Scientific data*, 5(1):1–9, 2018. [1](#), [2](#), [5](#)
- [57] Vladimir N Vapnik. An overview of statistical learning theory. *IEEE transactions on neural networks*, 10(5):988–999, 1999. [1](#), [2](#), [6](#)
- [58] Zhibo Wang, Xiaowei Dong, Henry Xue, Zhifei Zhang, Weifeng Chiu, Tao Wei, and Kui Ren. Fairness-aware adversarial perturbation towards bias mitigation for deployed deep models. In *Proceedings of the IEEE/CVF Conference on Computer Vision and Pattern Recognition*, pages 10379–10388, 2022. [2](#)
- [59] Sangdoon Yun, Dongyoon Han, Seong Joon Oh, Sanghyuk Chun, Junsuk Choe, and Youngjoon Yoo. Cutmix: Regularization strategy to train strong classifiers with localizable features. In *Proceedings of the IEEE/CVF international conference on computer vision*, pages 6023–6032, 2019. [5](#), [7](#)
- [60] Muhammad Bilal Zafar, Isabel Valera, Manuel Gomez Rogriguez, and Krishna P Gummadi. Fairness constraints: Mechanisms for fair classification. In *Artificial intelligence and statistics*, pages 962–970. PMLR, 2017. [2](#)
- [61] Brian Hu Zhang, Blake Lemoine, and Margaret Mitchell. Mitigating unwanted biases with adversarial learning. In *Proceedings of the 2018 AAAI/ACM Conference on AI, Ethics, and Society*, pages 335–340, 2018. [2](#)
- [62] Yi Zhang and Jitao Sang. Towards accuracy-fairness paradox: Adversarial example-based data augmentation for visual debiasing. In *Proceedings of the 28th ACM International Conference on Multimedia*, pages 4346–4354, 2020. [2](#)
- [63] Han Zhao, Amanda Coston, Tameem Adel, and Geoffrey J Gordon. Conditional learning of fair representations. *arXiv preprint arXiv:1910.07162*, 2019. [1](#), [2](#)
- [64] Yongshuo Zong, Yongxin Yang, and Timothy Hospedales. Medfair: Benchmarking fairness for medical imaging. *arXiv preprint arXiv:2210.01725*, 2022. [1](#), [2](#), [5](#), [7](#)

Fair Distillation: Teaching Fairness from Biased Teachers in Medical Imaging

Supplementary Material

6. Data Pre-processing

The data preprocessing in this work follows the approach outlined in [64]. For data splitting. The dataset is randomly partitioned into training, validation, and testing sets, maintaining an 80/10/10 ratio unless stated otherwise. We then binarize both the prediction labels and sensitive attributes. Further details on this process are provided in the next section.

7. Dataset Details

In this section, we provide details about the datasets. All datasets are publicly available and can be accessed through the URLs listed in Table 4. The dataset statistics are provided in Table 5. Additionally, we summarize the statistics for the subgroups and class labels in Tables 6 through 10.

7.1. Sensitive Attributes

For the classification datasets, the sensitive attributes are defined as follows:

- **Skin Type:** For the sensitive attribute of skin type in Fitzpatrick17k, we divided the data into two groups. The first group includes samples with skin types ranging from 0 to 2, while the second group consists of samples with skin types above 2.
- **Age:** For HAM10000, PAPILA, CheXpert, and MIMIC-CXR datasets, we classified the sensitive attribute of age into two distinct categories: the first group includes individuals aged 0 to 60, while the second group consists of those older than 60.
- **Race:** For CheXpert and MIMIC-CXR datasets, we defined two groups of race: a non-White group, comprising patients identified as 'Black' or 'Asian,' and a second group of patients identified as 'White'.
- **Gender:** For HAM10000, PAPILA, CheXpert, and MIMIC-CXR datasets, the sensitive attribute of gender has two categories: the first group consists of 'Male' patients, while the second group includes 'Female' patients.

The Harvard-FairSeg dataset [54] encompasses six distinct sensitive attributes. Specifically, regarding racial demographics, it includes samples from three primary groups: Asian (919 samples), Black (1,473 samples), and White (7,608 samples). Gender distribution shows that females represent 58.5% of subjects, with males comprising the remaining 41.5%. Ethnically, 90.6% of participants are Non-Hispanic, 3.7% are Hispanic, and 5.7% are unspecified. For preferred language, 92.4% of individuals prefer English, 1.5% prefer Spanish, 1% prefer other languages, and 5.1%

have no specified language preference. Regarding marital status, 57.7% are married or partnered, 27.1% are single, 6.8% are divorced, 0.8% are legally separated, 5.2% are widowed, and 2.4% did not specify. In this study, we focus on the three sensitive attributes with the highest observed group-wise disparities: race, gender, and ethnicity.

7.2. Disease Labels

- **Fitzpatrick17k:** We grouped the three partition labels into binary categories, namely *benign* and *malignant*. In this grouping, we classified both *non-neoplastic* and *benign* under the benign category, while *malignant* remained as the malignant category. Furthermore, we used Fitzpatrick skin type labels as the sensitive attributes for our analysis.
- **HAM10000:** We followed the approach by [34] to categorize the seven diagnostic labels into two binary groups: *benign* and *malignant*.
 - The *benign* group includes basal cell carcinoma (`bcc`), benign keratosis-like lesions (e.g., solar lentigines, seborrheic keratoses, and lichen-planus-like keratoses, `bk1l`), dermatofibroma (`df`), melanocytic nevi (`nv`), and vascular lesions (angiomas, angiokeratomas, pyogenic granulomas, and hemorrhage, `vasc`).
 - The *malignant* group consists of actinic keratoses and intraepithelial carcinoma (Bowen's disease, `akiec`) as well as melanoma (`mel`).

Images without recorded sensitive attributes were excluded from the dataset, leaving a total of 9,948 images.

- **PAPILA:** In this dataset, we excluded the *suspect* label class and focused on a binary classification task, using only images labeled as either *glaucomatous* or *non-glaucomatous*. The dataset contains both right-eye and left-eye images from the same patients. To divide the dataset into training, validation, and test sets, we followed a specific ratio: 70% for training, 10% for validation, and 20% for testing. Importantly, we ensured that images from the same patient are not shared across these splits. This practice preserves the independence of the data subsets, which is essential for accurately evaluating the model's performance.
- **CheXpert:** This dataset comprises 224,316 chest radiographs from 65,240 patients. Each image may be assigned one or more labels from a set of 14, representing various clinical observations. During preprocessing, we excluded images that lacked sensitive attribute labels. The *No Finding* label is utilized for both training and testing purposes. All available frontal and lateral images were included, ensuring that images from the same pa-

Table 4. Access information for datasets used in the experiments.

Dataset	Access
Fitzpatrick17k	https://github.com/mattgroh/fitzpatrick17k
HAM10000	https://dataverse.harvard.edu/dataset.xhtml?persistentId=doi:10.7910/DVN/DBW86T
PAPILA	https://www.nature.com/articles/s41597-022-01388-1#Sec6
CheXpert	Original data: https://stanfordmlgroup.github.io/competitions/chexpert/ Demographic data: https://stanfordaimi.azurewebsites.net/datasets/192ada7c-4d43-466e-b8bb-b81992bb80cf
MIMIC-CXR	https://physionet.org/content/mimic-cxr-jpg/2.0.0/

Table 5. Dataset statistics including imaging modality, the number of images, and sensitive attributes.

Dataset	Imaging Modality	Number of Images	Sensitive Attribute
Fitzpatrick17k	Skin Dermatology (2D)	16,012	Skin Type
HAM10000	Skin Dermatology (2D)	9,948	Age, Gender
PAPILA	Fundus Image (2D)	420	Age, Gender
CheXpert	Chest Radiographs (2D)	222,793	Age, Gender, Race
MIMIC-CXR	Chest Radiographs (2D)	370,955	Age, Gender, Race

Table 6. Label Distribution by Sensitive Attribute for the HAM10000 Dataset

Attribute	Label 0 (Healthy)	Label 1 (Unhealthy)	Total
Male	4492	908	5400
Female	4018	530	4548
Age Group 0	6465	684	7149
Age Group 1	2045	754	2799

Table 7. Label Distribution by Sensitive Attribute for the PAPILA Dataset

Attribute	Label 0 (Healthy)	Label 1 (Unhealthy)	Total
Male	111	35	146
Female	222	52	274
Age Group 0	163	15	178
Age Group 1	170	72	242

Table 8. Label Distribution by Sensitive Attribute for the Fitzpatrick17k Dataset

Attribute	Label 0 (Healthy)	Label 1 (Unhealthy)	Total
Skin Type 0	9412	1651	11063
Skin Type 1	4440	509	4949

tient were not shared across the training, validation, and test sets, following the approach outlined by [64].

- **MIMIC-CXR:** Race data is sourced from the MIMIC-IV dataset [19], which is hosted in the PhysioNet database [10]. We merged this data with the original MIMIC-CXR metadata using the *subject ID* as the key. Other preprocessing steps closely follow the procedures used in the CheXpert dataset.

Table 9. Label Distribution by Sensitive Attribute for the CheXpert Dataset

Attribute	Label 0 (Healthy)	Label 1 (Unhealthy)	Total
Male	13,062	119,143	132,205
Female	9,177	81,411	90,588
Age Group 0	16,274	90,488	106,762
Age Group 1	7,160	108,871	116,031
White	12,538	113,095	125,633
Non-White	9,794	87,366	97,160

Table 10. Label Distribution by Sensitive Attribute for the MIMIC-CXR Dataset

Attribute	Label 0 (Healthy)	Label 1 (Unhealthy)	Total
Male	72,297	121,168	193,465
Female	76,113	101,377	177,490
Age Group 0	63,072	45,407	108,479
Age Group 1	72,419	190,057	262,476
White	78,193	146,403	224,596
Non-White	70,211	76,148	146,359

8. Fairness Measures

For the classification metrics, the ES-AUC provides an equity-focused assessment by scaling the overall AUC based on performance differences across subgroups, calculated as follows:

$$ES - AUC = \frac{AUC(\mathcal{D})}{1 + \frac{1}{A} \sum_{g \in \mathcal{A}} |AUC(\mathcal{D}) - AUC(\mathcal{D}_g)|} \quad (4)$$

where $AUC(\mathcal{D})$ represents the overall AUC for the whole test set, $g \in \mathcal{A} \subset \{0, \dots, A\}$ represents the value of the identity attribute (e.g., for the gender attribute, the values can be male or female), $AUC(\mathcal{D}_g)$ represents the cohort-specific AUC on the test set $\mathcal{D}_g = \{(x, y, a) | (x, y, a) \in \mathcal{D}, a = g\}$ defined in (2). This measure promotes fairness by proportionally reducing the overall AUC in response to increased subgroup disparities.

The Performance-Scaled Disparity (PSD) evaluates fairness by comparing cohort performance relative to overall AUC. Mean PSD calculates the standard deviation of AUC scores across cohorts, while Max PSD calculates the maximum absolute difference between cohorts' AUCs, both scaled by the overall AUC. These metrics are defined as follows:

$$MeanPSD = \frac{\sqrt{\frac{1}{A} \sum_{g \in \mathcal{A}} (AUC(\mathcal{D}_g) - AUC_{mean})^2}}{AUC(\mathcal{D})}, \quad (5)$$

where $AUC_{mean} = \frac{1}{A} \sum_{g \in \mathcal{A}} AUC(\mathcal{D}_g)$, and

$$MaxPSD = \frac{(\max_{g \in \mathcal{A}}(AUC(\mathcal{D}_g)) - \min_{g \in \mathcal{A}}(AUC(\mathcal{D}_g)))}{AUC(\mathcal{D})}. \quad (6)$$

These PSD measures provide interpretable insights into the model’s fairness performance, especially in clinical contexts where consistent accuracy across demographic groups is essential.

For the segmentation measures, the Dice coefficient is calculated as [6, 51]

$$\text{Dice}(y, \hat{y}) = \frac{2 \times |y \cap \hat{y}|}{|y| + |\hat{y}|}, \quad (7)$$

where y and \hat{y} represent the actual and predicted segmented pixels, respectively. The Intersection over Union (IoU) [18] is given by

$$\text{IoU}(y, \hat{y}) = \frac{|y \cap \hat{y}|}{|y \cup \hat{y}|}. \quad (8)$$

Both metrics range from 0 to 1, with 1 indicating perfect overlap, but Dice tends to be slightly more sensitive to small overlaps than IoU due to its formula. To adapt Dice to penalize discrepancies in performance across demographic groups, we first define a performance discrepancy as follows:

$$\Delta(y, \hat{y}) = \sum_{g \in \mathcal{A}} |\text{Dice}(y, \hat{y}) - \text{Dice}(y, \hat{y}; g)|, \quad (9)$$

where $\text{Dice}(y, \hat{y}; g)$ measures Dice for samples belonging to a particular value $g \in \mathcal{A}$. The metric $\Delta(y, \hat{y})$ quantifies the deviation in performance of each demographic group relative to the overall performance, approaching zero when all groups achieve comparable segmentation accuracy. To evaluate fairness across different groups, we compute the relative disparity between the overall segmentation accuracy and the accuracy within each demographic group. The Equity-Scaled Dice (ES-Dice) metric is then defined as:

$$\text{ES} - \text{Dice}(y, \hat{y}) = \frac{\text{Dice}(y, \hat{y})}{1 + \Delta(y, \hat{y})}. \quad (10)$$

This formulation ensures that $\text{ES} - \text{Dice}(\cdot)$ is always less than or equal to 1. As Δ decreases (indicating more equitable segmentation performance across groups), $\text{ES} - \text{Dice}(\cdot)$ converges to $\text{Dice}(\cdot)$. Conversely, a higher Δ reflects greater disparity in segmentation performance across demographics, leading to a lower $\text{ES} - \text{Dice}(\cdot)$ score. This approach enables us to assess segmentation models not only for accuracy (measured by Dice) but also for fairness across demographic groups. Note that the calculation of $\text{ES} - \text{IoU}(\cdot)$ follows the same steps as defined in (9) and (10).

9. Complete Set of Results

Tab. 11 shows the complete set of classification results, while Tabs. 12 to 14 show a complete set of segmentation results.

Table 11. Complete evaluation of fairness **classification** models across medical imaging benchmarks: HAM10000, Fitzpatrick17k, PAPANILA, CheXpert, and MIMIC-CXR. We report overall AUC, subgroup-minimum AUC, ES-AUC, AUC gap, MeanPSD, and MaxPSD. Best results are highlighted.

Dataset	Attr.	Metric	ERM	GroupDRO	SWAD	FIS	FairDi (Ours)
HAM10000	Age	Overall AUC \uparrow	0.9000	0.8932	0.8961	0.9220	0.9447
		Min. AUC \uparrow	0.7753	0.8000	0.8666	0.8832	0.9266
		ES-AUC \uparrow	0.8383	0.8386	0.8712	0.9045	0.9353
		AUC Gap \downarrow	0.1472	0.1301	0.0572	0.0388	0.0201
		Mean PSD \downarrow	8.18×10^{-2}	7.28×10^{-2}	3.19×10^{-2}	2.42×10^{-2}	1.06×10^{-2}
		Max PSD \downarrow	1.64×10^{-1}	1.46×10^{-1}	6.38×10^{-2}	4.85×10^{-2}	2.13×10^{-2}
	Gender	Overall AUC \uparrow	0.8520	0.8703	0.9144	0.9300	0.9560
		Min. AUC \uparrow	0.8312	0.8592	0.9114	0.9276	0.9553
		ES-AUC \uparrow	0.8381	0.8625	0.9124	0.9283	0.9553
		AUC Gap \downarrow	0.0331	0.0180	0.0044	0.0011	0.000029
		Mean PSD \downarrow	1.94×10^{-2}	1.03×10^{-2}	2.41×10^{-3}	5.77×10^{-4}	1.52×10^{-5}
		Max PSD \downarrow	3.88×10^{-2}	2.07×10^{-2}	4.81×10^{-3}	1.15×10^{-3}	3.03×10^{-5}
Fitzpatrick17k	Skin Type	Overall AUC \uparrow	0.9151	0.9198	0.9331	0.9023	0.9417
		Min. AUC \uparrow	0.9067	0.8997	0.9094	0.8956	0.9406
		ES-AUC \uparrow	0.8985	0.8943	0.9026	0.8895	0.9408
		AUC Gap \downarrow	0.0370	0.0571	0.0675	0.0287	0.0020
		Mean PSD \downarrow	2.02×10^{-2}	3.10×10^{-2}	3.62×10^{-2}	1.59×10^{-2}	1.10×10^{-3}
		Max PSD \downarrow	4.04×10^{-2}	6.21×10^{-2}	7.23×10^{-2}	3.17×10^{-2}	2.21×10^{-3}
PAPILA	Age	Overall AUC \uparrow	0.6498	0.7565	0.8227	0.9437	0.9807
		Min. AUC \uparrow	0.5322	0.5826	0.6639	0.9168	0.9806
		ES-AUC \uparrow	0.5779	0.6259	0.7043	0.9194	0.9713
		AUC Gap \downarrow	0.2490	0.4174	0.3361	0.0528	0.0194
		Mean PSD \downarrow	1.92×10^{-1}	2.76×10^{-1}	2.04×10^{-1}	2.80×10^{-2}	9.89×10^{-3}
		Max PSD \downarrow	3.83×10^{-1}	5.52×10^{-1}	4.09×10^{-1}	5.60×10^{-2}	1.98×10^{-2}
	Gender	Overall AUC \uparrow	0.7840	0.7969	0.7666	0.9391	0.9572
		Min. AUC \uparrow	0.7804	0.7917	0.6667	0.9186	0.9508
		ES-AUC \uparrow	0.7815	0.7921	0.7096	0.9259	0.9408
		AUC Gap \downarrow	0.0008	0.0122	0.1608	0.0285	0.0349
		Mean PSD \downarrow	5.10×10^{-4}	7.65×10^{-3}	1.05×10^{-1}	1.52×10^{-2}	1.82×10^{-2}
		Max PSD \downarrow	1.02×10^{-3}	1.53×10^{-2}	2.10×10^{-1}	3.03×10^{-2}	3.64×10^{-2}
CheXpert	Age	Overall AUC \uparrow	0.8809	0.8493	0.8875	0.8727	0.8735
		Min. AUC \uparrow	0.7836	0.7991	0.8454	0.8464	0.8502
		ES-AUC \uparrow	0.8376	0.8240	0.8667	0.8611	0.8614
		AUC Gap \downarrow	0.1033	0.0613	0.0479	0.0256	0.0281
		Mean PSD \downarrow	5.86×10^{-2}	3.61×10^{-2}	2.70×10^{-2}	1.47×10^{-2}	1.61×10^{-2}
		Max PSD \downarrow	1.17×10^{-1}	7.22×10^{-2}	5.40×10^{-2}	2.93×10^{-2}	3.22×10^{-2}
	Gender	Overall AUC \uparrow	0.8809	0.8627	0.8879	0.8752	0.8797
		Min. AUC \uparrow	0.8807	0.8624	0.8872	0.8705	0.8768
		ES-AUC \uparrow	0.8808	0.8624	0.8873	0.8699	0.8765
		AUC Gap \downarrow	0.0002	0.0006	0.0013	0.0121	0.0074
		Mean PSD \downarrow	1.14×10^{-4}	3.48×10^{-4}	7.32×10^{-4}	6.95×10^{-3}	4.24×10^{-3}
		Max PSD \downarrow	2.27×10^{-4}	6.95×10^{-4}	1.46×10^{-3}	1.39×10^{-2}	8.48×10^{-3}
Race	Overall AUC \uparrow	0.8792	0.8630	0.8875	0.8665	0.8788	
	Min. AUC \uparrow	0.8784	0.8599	0.8865	0.8616	0.8783	
	ES-AUC \uparrow	0.8785	0.8602	0.8866	0.8605	0.8784	
	AUC Gap \downarrow	0.0016	0.0065	0.0021	0.014	0.0010	
	Mean PSD \downarrow	9.10×10^{-4}	3.77×10^{-3}	1.18×10^{-3}	8.08×10^{-3}	5.82×10^{-4}	
	Max PSD \downarrow	1.82×10^{-3}	7.53×10^{-3}	2.37×10^{-3}	1.62×10^{-2}	1.16×10^{-3}	
MIMIC-CXR	Age	Overall AUC \uparrow	0.8640	0.8349	0.8708	0.8753	0.8793
		Min. AUC \uparrow	0.8106	0.7862	0.8215	0.8469	0.8555
		ES-AUC \uparrow	0.8414	0.8130	0.8491	0.8562	0.8629
		AUC Gap \downarrow	0.0532	0.0538	0.0510	0.0446	0.0381
		Mean PSD \downarrow	3.08×10^{-2}	3.22×10^{-2}	2.93×10^{-2}	2.55×10^{-2}	2.17×10^{-2}
		Max PSD \downarrow	6.16×10^{-2}	6.44×10^{-2}	5.86×10^{-2}	5.10×10^{-2}	4.33×10^{-2}
	Gender	Overall AUC \uparrow	0.8645	0.8589	0.8705	0.8681	0.8776
		Min. AUC \uparrow	0.8562	0.8496	0.8623	0.8580	0.8689
		ES-AUC \uparrow	0.8584	0.8520	0.8645	0.8607	0.8710
		AUC Gap \downarrow	0.0141	0.0161	0.0139	0.0173	0.0152
		Mean PSD \downarrow	8.16×10^{-3}	9.37×10^{-3}	7.98×10^{-3}	9.96×10^{-3}	8.66×10^{-3}
		Max PSD \downarrow	1.63×10^{-2}	1.87×10^{-2}	1.60×10^{-2}	1.99×10^{-2}	1.73×10^{-2}
Race	Overall AUC \uparrow	0.8626	0.8565	0.8710	0.8787	0.8811	
	Min. AUC \uparrow	0.8552	0.8490	0.8638	0.8709	0.8714	
	ES-AUC \uparrow	0.8589	0.8531	0.8672	0.8742	0.8741	
	AUC Gap \downarrow	0.0085	0.0080	0.0088	0.0103	0.0160	
	Mean PSD \downarrow	4.93×10^{-3}	4.67×10^{-3}	5.05×10^{-3}	5.86×10^{-3}	9.08×10^{-3}	
	Max PSD \downarrow	9.85×10^{-3}	9.34×10^{-3}	1.01×10^{-2}	1.17×10^{-2}	1.82×10^{-2}	

Table 12. **Segmentation** performance for optic cup and rim on the Harvard-FairSeg dataset, with **race** as the sensitive attribute.

Method	Overall ES-Dice \uparrow	Overall Dice \uparrow	Overall ES-IoU \uparrow	Overall IoU \uparrow	Asian Dice \uparrow	Black Dice \uparrow	White Dice \uparrow	Asian IoU \uparrow	Black IoU \uparrow	White IoU \uparrow	
Cup	TransUNet	0.8281	0.8481	0.7300	0.7532	0.8270	0.8489	0.8503	0.7277	0.7576	0.7551
	TransUNet+ADV	0.8256	0.8410	0.7265	0.7432	0.8246	0.8417	0.8426	0.7260	0.7482	0.7440
	TransUNet+GroupDRO	0.8201	0.8442	0.7252	0.7479	0.8197	0.8469	0.8464	0.7232	0.7529	0.7495
	TransUNet+FEBS	0.8253	0.8464	0.7265	0.7497	0.8248	0.8484	0.8484	0.7247	0.7550	0.7513
	TransUNet+FairDi	0.8386	0.8532	0.7365	0.7543	0.8386	0.8527	0.8555	0.7359	0.7552	0.7591
Rim	TransUNet	0.7034	0.7927	0.5848	0.6706	0.7457	0.7307	0.8106	0.6160	0.5991	0.6913
	TransUNet+ADV	0.7000	0.7906	0.5825	0.6682	0.7413	0.7286	0.8087	0.6116	0.5982	0.6888
	TransUNet+GroupDRO	0.7002	0.7896	0.5814	0.6674	0.7470	0.7229	0.8080	0.6183	0.5899	0.6887
	TransUNet+FEBS	0.7050	0.7950	0.5871	0.6725	0.7479	0.7325	0.8130	0.6185	0.6020	0.6935
	TransUNet+FairDi	0.7278	0.8027	0.5994	0.6828	0.7533	0.7492	0.8027	0.6235	0.6128	0.6927

Table 13. **Segmentation** performance for optic cup and rim on the Harvard-FairSeg dataset, with **gender** as the sensitive attribute.

Method	Overall ES-Dice \uparrow	Overall Dice \uparrow	Overall ES-IoU \uparrow	Overall IoU \uparrow	Male Dice \uparrow	Female Dice \uparrow	Male IoU \uparrow	Female IoU \uparrow	
Cup	TransUNet	0.8435	0.8481	0.7490	0.7532	0.8458	0.8513	0.7508	0.7564
	TransUNet+ADV	0.8342	0.8345	0.7348	0.7356	0.8344	0.8348	0.7361	0.7350
	TransUNet+GroupDRO	0.8405	0.8478	0.7453	0.7522	0.8441	0.8528	0.7483	0.7575
	TransUNet+FEBS	0.8464	0.8489	0.7492	0.7530	0.8494	0.8514	0.7505	0.7556
	TransUNet+FairDi	0.8521	0.8535	0.7576	0.7623	0.8529	0.8545	0.7577	0.7639
Rim	TransUNet	0.7882	0.7927	0.6659	0.6706	0.7951	0.7894	0.6736	0.6665
	TransUNet+ADV	0.7754	0.7852	0.6522	0.6630	0.7905	0.7779	0.6699	0.6534
	TransUNet+GroupDRO	0.7893	0.7917	0.6673	0.6699	0.7930	0.7900	0.6716	0.6677
	TransUNet+FEBS	0.7851	0.7898	0.6655	0.6698	0.7924	0.7932	0.6678	0.6653
	TransUNet+FairDi	0.7917	0.7988	0.6742	0.6783	0.8016	0.7926	0.6792	0.6731

Table 14. **Segmentation** performance for optic cup and rim on the Harvard-FairSeg dataset, with **ethnicity** as the sensitive attribute.

Method	Overall ES-Dice \uparrow	Overall Dice \uparrow	Overall ES-IoU \uparrow	Overall IoU \uparrow	Hispanic Dice \uparrow	Non-Hispanic Dice \uparrow	Hispanic IoU \uparrow	Non-Hispanic IoU \uparrow	
Cup	TransUNet	0.8281	0.8481	0.7300	0.7532	0.8463	0.8704	0.7508	0.7826
	TransUNet+ADV	0.8112	0.8320	0.7083	0.7315	0.8304	0.8561	0.7294	0.7622
	TransUNet+GroupDRO	0.8332	0.8482	0.7358	0.7526	0.8468	0.8648	0.7507	0.7735
	TransUNet+FEBS	0.8320	0.8483	0.7359	0.7542	0.8501	0.8661	0.7515	0.7764
	TransUNet+FairDi	0.8396	0.8516	0.7581	0.7683	0.8564	0.8611	0.7698	0.7803
Rim	TransUNet	0.7815	0.7927	0.6626	0.6706	0.7914	0.8057	0.6695	0.6815
	TransUNet+ADV	0.7774	0.7841	0.6557	0.6602	0.7829	0.7915	0.6590	0.6658
	TransUNet+GroupDRO	0.7904	0.7943	0.6672	0.6733	0.7936	0.7901	0.6728	0.6646
	TransUNet+FEBS	0.7857	0.7939	0.6692	0.6754	0.7943	0.8040	0.6697	0.6789
	TransUNet+FairDi	0.7871	0.7962	0.6755	0.6792	0.8068	0.7952	0.6784	0.6839